CellPress

Microfluidics for sperm research

Stephanie M. Knowlton[1], Magesh Sadasivam[2], and Savas Tasoglu[1,3]

[1] Department of Biomedical Engineering, University of Connecticut, 260 Glenbrook Road, Storrs, CT 06269, USA
[2] Helmholtz Zentrum München, Ingolstädter Landstraße 1, 85764, Oberschleißheim, Germany
[3] Department of Mechanical Engineering, University of Connecticut, 191 Auditorium Road, Storrs, CT 06269, USA

One in six couples of reproductive age worldwide are affected at least once by some form of infertility. *In vitro* fertilization (IVF) and intracytoplasmic sperm injection (ICSI) are widely-available assisted reproductive technologies (ART). The identification and isolation of the most-motile sperm with DNA integrity are essential to IVF and ICSI, ultimately affecting treatment consequences and the health of offspring. Recently, microfluidic technologies been developed to sort sperm according to sperm morphology, motility, DNA integrity, and functionality for IVF techniques. There have also been emerging applications in wildlife conservation, high-throughput single-sperm genomics, sperm-driven robotics, and in-home fertility testing. We review a broad range of studies applying the principles of microfluidics to sperm research.

Current need for sperm-sorting technologies

Infertility affects about 50–80 million couples worldwide, accounting for 8–12% of couples with women of reproductive age [1]. Male infertility contributes to about one half of infertility cases [2]. Most cases are due to low sperm count, which is commonly caused by primary testicular failure. Nutritional deficiencies, stress, chronic inflammation, and environmental exposure to particular toxins can also decrease sperm quantity and quality. Low sperm count, low sperm motility, and sperm abnormality impair the ability of sperm cells to fertilize an oocyte naturally [3]. Assisted reproductive technologies (ART) provide a set of powerful techniques to assist couples facing infertility issues. Intracytoplasmic sperm injection (ICSI) is an ART which currently serves as the standard for managing male-factor infertility given that it provides enhanced fertilization rates compared to other technologies, including traditional IVF [4,5]. Selection of highly-motile sperm is crucial to successful ICSI because fertilization of the oocyte and ultimately a viable birth depend largely on sperm quality [6–8]. Thus, technologies to facilitate identification and selection of healthy sperm can greatly improve the success rate of ICSI, IVF, and other ART.

Beyond clinical use, sperm sorting has also been applied to wildlife conservation efforts. Captive-breeding sex selection is important for wildlife species which naturally exist in female-dominated social groups, where it is important to maintain a sex ratio biased toward females to reduce male–male aggression and maintain socially unified groups [9]. Sperm sorting is also of interest for maintaining endangered species populations [9] or farm animal populations [10] because a bias toward production of females can help the population to reproduce at a faster rate. In addition, sperm sorting in-house with affordable, user-friendly devices would eliminate the need for multiple freeze–thaw cycles, which reduce viability in sperm samples [11], when sending samples to remote sperm-sorting facilities.

The field of microfluidics has been creating a significant surge in biomedical research in the past decade with many *in vitro* models closely simulating microenvironments in the human body [12–14]. In the 1990s the Defense Advanced Research Projects Agency (DARPA) allocated an enormous stimulus package to develop this technology as a diagnostic tool for resource-limited military field environments. The advent of novel micro- and nano-devices presents promising solutions to a wide range of clinical problems. The emerging importance of these technologies has yet to be fully realized in the burgeoning science of reproductive medicine. Recently, a range of studies have applied microfluidics to sperm sorting, representing significant progress for improving ART as well as wildlife conservation techniques. Microfluidics has also been utilized for high-throughput single-sperm genomics and has shown promise in sperm-driven robotics. There is also a potential for improving accuracy of in-home fertility tests using microfluidic devices. We review a broad range of studies on microfluidics applied to sperm sorting to address these challenges.

Technologies for sperm sorting

Conventional technologies

Selection of sperm for IVF and ICSI is generally based on sperm motility because highly motile sperm are more capable of fertilizing an oocyte. Traditional sperm-selection techniques include the swim-up and density gradient-based centrifugation methods [15,16]. The swim-up method enables motile sperm to move away from its cohort of sedimented sperm into freshly layered media; however, the technique produces a low yield of motile sperm. Density gradient-based centrifugation can select sperm cells based on their density; however, centrifugation has a negative effect on sperm viability and can result in sperm DNA fragmentation [17]. Furthermore, these traditional techniques fail for samples with low sperm counts (<4 million/ml, classified as oligospermia) [18], samples with low sperm

Corresponding author: Tasoglu, S. (savas@engr.uconn.edu).
Keywords: microfluidics; sperm sorting for infertility; point-of-care; sperm genomics; wildlife conservation; sperm-driven robotics.

0167-7799/
 http://dx.doi.org/10.1016/j.tibtech.2015.01.005

motility (oligospermaesthenia) [16], or cryopreserved samples of sperm with reduced motility [19]. Nevertheless, these compromising factors tend to predominate in semen samples which require ICSI, presenting a need for alternative methods of sperm selection. The microdrop technique is widely used as an alternative to the swim-up and density-gradient techniques to select motile sperm from low quality samples. In this procedure, sperm swimming to the periphery of a 50–100 μl media drop are manually separated for use in fertilization [20]. However, this technique is highly subjective and dependent on the skill of the embryologist, and this introduces human error into the process. Thus, technologies which can automate the sperm-selection process and be applied in a clinical setting will be necessary to improve the success rate of fertilization in cases of male-factor infertility.

Microfluidic technologies

Microfluidics has been widely utilized for various areas of research and for clinical applications including biological and chemical analysis [12,21,22], point-of-care testing [23–28], clinical and forensic analysis [29], molecular diagnostics, and medical diagnostics [30–35]. In this section we review microfluidic technologies for sperm sorting which utilize the principles of chemoattractant gradients, fluidic flow, and thermotactic forces (Figure 1A–C). In passively driven microfluidic technologies, none of these forces are present and the only driving force is sperm motility (Figure 1D). Current microfluidic technologies for sperm sorting are summarized in Table 1.

Passively driven microfluidics. In passively driven sorting, the fundamental idea is to collect the most-motile

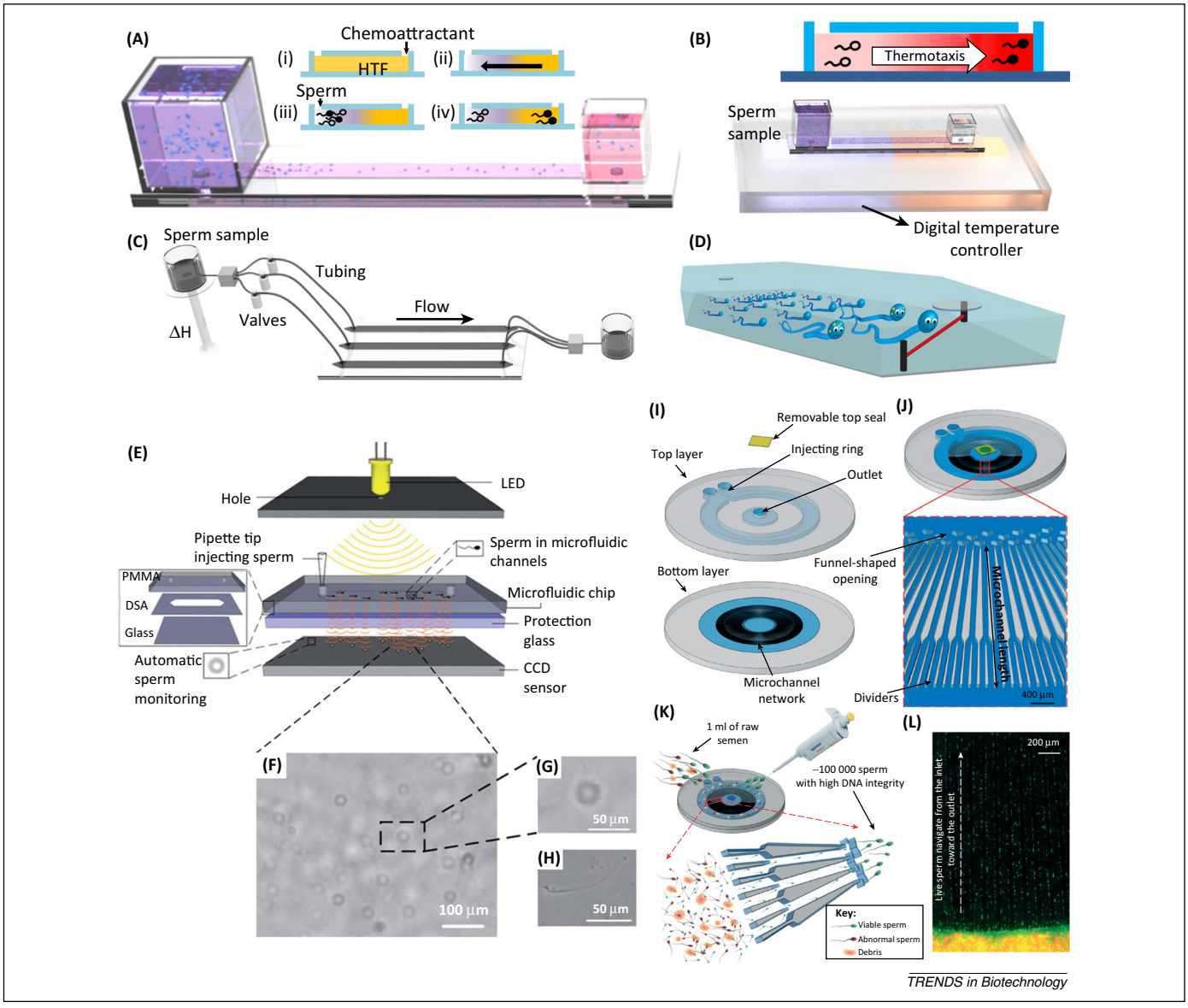

Figure 1. Illustration of present microfluidic technologies for sperm sorting which utilize the principles of **(A)** chemoattractant gradients, **(B)** thermotactic forces, and **(C)** fluidic flow. **(D)** In other microfluidic technologies, the only driving force is the self-motion of sperm. **(E)** A passively driven microfluidic chip integrated with a lensless charge-coupled device (CCD) to enable a larger field of view (FOV). **(F)** Shadow image of sperm obtained by the CCD camera. **(G)** The enlarged shadow image compared to **(H)** a 10× objective microscope image, both at 50 μm scale. Reproduced, with permission, from [36]. **(I)** A multiplexed microfluidic design showing input and outlet chambers. **(J)** Network of 500 radial microchannels. **(H)** Selective separation of viable sperm from abnormal sperm by microchannel design. **(L)** Fluorescent visualization of dead (red) and live (green) sperm separation. Reproduced, with permission, from [39].

Table 1. Present microfluidic technologies for sperm sorting

Principle	Setup	Medium	Sperm type	Sample amount	Imaging	Refs
Passively driven	PMMA-DSA-glass	HTF	Mouse	1 μl sperm solution	Lensless charge-coupled device (CCD)	[36]
Passively driven	PMMA-DSA-glass	HTF with BSA	Human, mouse	1 μl sperm solution (1500–4000 sperm)	CCD-coupled inverted microscope	[37]
Passively driven	PMMA-DSA-glass	HTF with 1% BSA	Human	560 μl raw semen or 1:4 diluted sample	CCD-coupled inverted microscope	[38]
Passively driven	PDMS-glass	HTF	Human, bull	1 ml raw semen	CCD-coupled inverted fluorescence microscope	[39]
Chemoattractant-driven (cumulus, acetylcholine)	Silicon-glass	HEPES-buffered HTF	Human	<2 μl raw semen	Cassette recorder-based B&W TV camera and microscope	[40]
Chemoattractant-driven (cumulus cells)	PDMS-glass	HTF	Mouse	Volume not specified (~ 25 000 sperm)	CCD-coupled inverted microscope	[41]
Chemoattractant-driven (oocyte)	PDMS-glass	HTF	Mouse	Volume not specified (~ 25 000 sperm)	CCD-coupled inverted microscope	[42]
Chemoattractant-driven (acetylcholine)	PDMS-glass	HTF	Mouse	1 μl sperm solution (~11 sperm)	CCD-coupled inverted microscope	[43]
Flow-driven	PDMS	HTF with 0.2% BSA	Human	50 μl washed semen	CCD-coupled inverted microscope	[44]
Flow-driven	PDMS	DPBS	Bull, mouse, human	20 μl sperm sample	Microscope and digital camera	[45]
Flow-driven	PDMS-glass	RPMI, seminal plasma	Human	200 μl raw semen	Electrical resistive pulse detection	[46]
Flow-driven	PDMS-glass	RPMI, 0.1% polyvinyl alcohol, 3% BSA	Human	2.3 μl raw semen	Microscope and digital camera	[47]
Thermotaxis	PDMS	HTF	Human	0.5 μl sperm sample ($2.5–20\times10^3$ sperm)	CCD-coupled inverted microscope	[48]
Combined: pressure- and chemoattractant-driven	PDMS-glass	1% PBS, 1% (w/v) BSA	Mouse	Volume not specified	CCD-coupled inverted microscope	[49]

sperm from the outlet of microfluidic channels at an optimized time-point while less-motile or immotile sperm are left behind in the microchannels. To track a large number of sperm simultaneously and address the challenges associated with the small field of view (FOV) of conventional microscopic imaging, a microfluidic chip was integrated with a lensless charge-coupled device (CCD) [36]. The integrated microfluidic platform enabled tracking of sperm and their motilities by tracing their shadow paths in the microfluidic channel. Microchannels and sperm motion were monitored in a larger FOV in both vertical configuration (akin to the conventional swim-up column method) and horizontal configuration (Figure 1E–H). The platform was able to detect higher motility in the outlet of the microfluidic chip, and lower motility in the inlet, relative to the motility of non-sorted samples.

A coarse-grained computational model was developed to better understand the underlying principles of sperm motion and exhaustion in microfluidic channels. Computational results were matched with the experimental results of passively driven sperm sorting in a microfluidic design [37]. Both human and mouse sperm motion were quantitatively evaluated. Computational results indicated a significant role of mouse sperm exhaustion during sorting. Experimental results matched well with the computational model with an average exhaustion time of 30 minutes for mouse sperm. For human sperm (up to 1 h incubation), the exhaustion time in the computational model did not play a significant role, indicating longer exhaustion times of human sperm.

More recently, passively driven microfluidic techniques have been developed to process raw semen. One microfluidic chip was recently presented to sort and collect motile, healthy, and morphologically normal sperm from raw unprocessed semen without centrifugation [38]. The design consists of a single channel and a retrieval chamber with a polycarbonate membrane filter. This method resulted in a higher percentage of sorted sperm with retained DNA integrity and fewer reactive oxygen species compared to samples sorted using the conventional swim-up method. In another study, a microfluidic platform with 500 parallel microchannels was developed to sort sperm based on progressive motility (Figure 1I–L) [39]. Raw semen was used as the input, and semen purification and high DNA integrity sperm selection were completed in a one-step procedure in under 20 minutes. These results showed >89% improvement in bull sperm vitality and 80% improvement in human sperm DNA integrity compared to samples sorted with conventional techniques.

Chemoattractant-driven microfluidics. *In vivo*, substances released from the egg form a gradient of bioactive residues in the oviduct as sperm cells swim toward an egg. Inspired by this naturally occurring phenomenon, chemoattractant-driven sperm sorting involves collection of the most responsive sperm from the outlet of microfluidic channels at an optimized time. In 1993, chemoattractant-driven sperm sorting was achieved in microchannels by utilizing microcompartments filled with either hyaluronic acid or cervical mucus [40]. Multiplexed evaluation of different spermicides such as nonoxynol-9 and C13G and concentrations of spermicide was performed. Samples were also evaluated for the presence of sperm-specific antibodies by employing human anti-IgG antibody-coated beads. Results highlighted the advantages of multiplexed sperm

evaluation over testing multiple features individually by employing an aging sample in conventional serial testing.

Since this work, more recent developments in chemoattractant-driven microfluidic devices have been made in the field of sperm sorting. One such device has been designed for combined monitoring of sperm chemotaxis and motility [41]. The design was composed of a straight channel with two branches mimicking the mammalian reproductive tract. Dimensions of the straight channel were optimized to maximize sperm motility in the outlet (motile sperm percentage in total sperm population) and relative sperm count in outlet pool (outlet sperm count normalized to the corresponding inlet sperm count). Mouse cumulus cells were seeded at the end of the branches on the opposite end of the sample insertion point to create a gradient of chemoattractant. Chemotaxis index was quantified as the ratio of the number of sperm swimming toward the end of one branch (pool A) versus the other branch (pool B). To statistically evaluate the effect of chemoattractant on sperm motion, four cases were studied: chemoattractant gradient in (i) the first branch, (ii) the second branch, (iii) both branches, and (iv) neither branch. In this study, ~10% of sperm were responsive to the chemoattractant gradient, showing a preference toward the cell-seeded branch.

Another microdevice has been presented to perform each step of IVF, including oocyte positioning, fertilization, embryo culture, and sperm screening (Figure 2E) [42]. Oocytes were individually positioned in a 4×4 matrix of cylindrical units located at the intersection of two perpendicular microchannels, which enabled effective motile sperm separation and fast suspension-medium replacement. Fertilization and early embryonic development were monitored by *in situ* fluorescent staining and analyzed. The motility of murine sperm was improved from 61% in

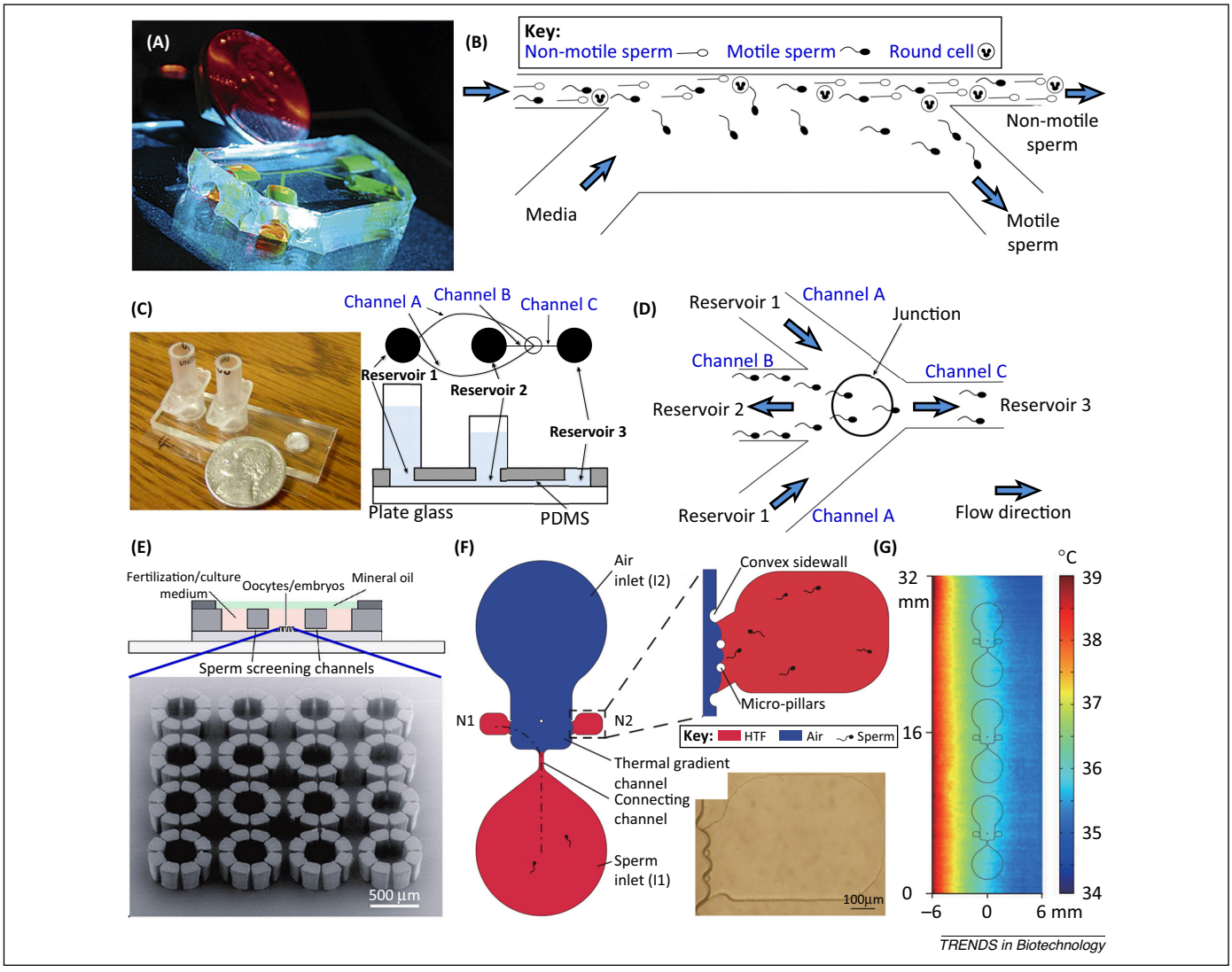

Figure 2. **(A)** A compact, simple, and disposable device for passively driven sperm sorting. **(B)** Fluid flow is used to sort sperm based on their ability to cross the passively driven laminar fluid stream created by a hydrostatic pressure difference between inlet and outlet. Reproduced, with permission, from [44]. **(C)** The compact, passively driven microfluidic device with a side view and top view schematic of the generation of hydrostatic pressure differences. **(D)** The junction showing sperm movement from input (reservoir 2) to outlet (reservoir 3). Reproduced, with permission, from [45]. **(E)** Schematic of the microfluidic IVF device. The oocytes are cultured at the center where four sperm-sorting channels intersect. Scanning electron micrograph of the 4×4 array of cylindrical units for single oocytes. Reproduced, with permission, from [42]. **(F)** An interfacial valve-based microfluidic chip for thermotactic evaluation of human sperm. The inlay and microscopic image show the air inlet used to close the interfacial valve, resulting in sperm being trapped in the branches. **(G)** Thermal gradient formed using a control unit between the branches, N1 and N2, of the devices. Reproduced, with permission, from [48].

the input region to 96% in the oocyte region. The rates of embryo growth and blastocyst formation in the microfluidic platform were comparable to those in Petri dishes. The healthy blastocysts obtained in the microfluidic platform may be conveniently retrieved by pipetting for clinical embryo transfer. These results showed great promise for microfluidic platforms that merge techniques of sperm and oocyte manipulation in a single unit.

More recently, another PDMS-glass microfluidic design was developed for selection and separation of progressive motile sperm from immotile sperm by utilizing acetylcholine as a chemoattractant [43]. The design was composed of eight channels extending radially from a circular inlet, each with a diffusion-generated gradient of acetylcholine with a different steepness. Three cases were studied: (i) distilled water (DW) was pipetted into every outlet, (ii) chemoattractant was pipetted into outlet 5, with DW in the other outlets, and (iii) DW was pipetted into outlet 5, with chemoattractant in the other outlets. The results demonstrated an optimal chemoattractant gradient of 0.625 (mg/ml)/mm for predominant sperm motion toward the outlet. Based on these findings, motile sperm specifically responded to the acetylcholine gradient, and the purity of the sorted samples was nearly 100%.

Flow-driven microfluidics. A microfluidic system was developed to sort sperm based on their motility and ability to cross streamlines in a laminar fluid stream (Figure 2A,B) [44]. The flow stream is driven passively by a constant hydraulic pressure initiated by capillary forces and gravity, eliminating the need for an external power source or control. The device isolated motile sperm from non-motile sperm and other cellular debris based on the ability of motile sperm to swim out of the fluid stream. These methods were shown to sort samples with nearly 100% purity of motile sperm, independently of the initial purity. There was also an observed improvement in morphology in sorted samples compared to that of unsorted samples.

Another microfluidic platform was presented which enables separation of motile and non-motile sperm, and control over sperm orientation, by using the self-movement of sperm against microfluidic flow created by a hydrostatic pressure difference between the inlet and outlet (Figure 2C,D) [45]. The design consists of four channels and three chambers: the pressure values at chambers 1 and 2 were initially equal, but the pressure at chamber 3 was lower (<1 mm height) compared to the others. A 20 μl sperm sample was loaded into reservoir 2. The pressure at reservoir 1 was increased by adding 20-40 μl of medium (about 1.14–2.28 mm height) at a time while monitoring sperm motility in the microchannel. As the fluid in microchannel B flows from right to left, the motile sperm cells swim from left to right. When motile sperm arrive at the junction, they are swept into channel C by a higher velocity flow and gather in chamber 3. Velocities of the motile sperm and the non-motile sperm/debris were quantified for a range of pressure differences and for three different species: human, bull, and mouse. Results verify that sperm swim against microflow created by hydrostatic pressure difference, and that this phenomenon can be leveraged to separate motile and non-motile sperm.

More recently, a flow-driven microfluidic device with three interconnecting channels was designed to separate and count sperm which are able overcome a fluid flow field within a specified time [46]. Fluid flows from channel A at a maximum velocity of 120 μm/s and splits into channels B and C. Semen is loaded into reservoir B and enters channel B against a parabolic flow of 40 μm/s maximum velocity. Sperm with sufficient velocity to overcome this flow and swim up the length of channel B within 12 minutes are flushed into channel C. An aperture in channel C serves as an electrical detector, and as motile sperm are flushed through channel C they are counted using a resistive pulse technique to quantify progressively motile sperm concentration.

Another device was developed to measure total and motile sperm counts using a two-channel design in which two channels, one filled with raw semen and the other with pure buffer, are separated by a permeative phase-guide structure [47]. Non-motile sperm remain in the input channel, while about half of the motile sperm swim across the barrier into the buffer channel. The sperm in each channel were agglomerated via centrifugation, and the pellet areas were quantified as a measure of total and motile sperm concentrations.

Thermotaxis-driven microfluidics. Thermotaxis has been demonstrated to be a significant factor in sperm quality assessment. Thermotactic assessment of human sperm was recently performed employing a microfluidic system with an interfacial valve (Figure 2F,G) [48]. A thermal gradient was created between two branches and precisely controlled by a peripheral temperature gradient control unit. Thermal gradient-responsive sperm gathered into the higher-temperature branch whereas non-responsive sperm swam non-preferentially toward both branches. Air–liquid interface valves were utilized to isolate the branches, enabling control of the entrapped sperm. Thermotactic force-based responses were observed in 6–11% of motile sperm using multiple temperature ranges starting at 34°, 35°, 36°, and 37°, and increasing by 1.3°C.

Multi-principle-driven microfluidics. A microfluidic device was presented to measure sperm chemotaxis by using the combination of shear flow and chemoattractant-based gradients [49]. The microfluidic setup utilized channels with a spatiotemporally stable gradient of chemoattractant. Mouse sperm were loaded into a reservoir between confluent flows of mouse ovary extract and suspension buffer. Four of six sperm moved toward the chemoattractant stream as a result of chemotaxis, while others swam non-preferentially in the buffer and chemoattractant streams. Quantification of chemotaxis was performed by counting chemoattractant-responsive sperm relative to those that moved toward the suspension buffer.

What does the field of microfluidics hold for *in vitro* sperm research?

PMMA/PDMS-based microfluidic chips with a glass substrate enable direct microscopic imaging of the sample. Although these chips are convenient for sperm research, there remain some shortcomings, such as the thickness of these chips and the need for specialized instruments for

chip fabrication. Hence, paper-based microfluidic chips are being investigated as a cheaper alternative. Earlier versions of paper microfluidic chips were opaque cellulose-based chips. However, these devices fall short when there is need for optical microscopic imaging necessitating an optical window specifically for imaging purposes [50]. Optically transparent paper-based chips (OTC) are chemically and biologically compatible, and they are able to easily accommodate fluid flow with capabilities comparable to, if not better than, PMMA/PDMS-based chips. OTC can easily accommodate high-throughput on-chip imaging technologies, making it a clear choice for point-of-care sperm-analysis applications. Chip-based imaging technologies are described in Box 2 and summarized in Table 2.

Less-expensive alternatives will enable a product to better reach a wide demographic of patients worldwide. As stated earlier, around half of the infertility problems arise from male-factor infertility [2]. In these cases, microfluidics can help to improve the quality of sperm samples used for ART by sorting sperm based on DNA integrity and progressive motility, both major factors affecting sperm quality. The sample may be manipulated and customized to suit various ARTs. For example, the ejaculate can be washed and the healthy sperm can be separated from debris, leukocytes, and other cellular plasma material. Microfluidic techniques show great potential in significantly reducing the risk ratio and in improving the success rate of ART [44,51].

Another crucial factor for the future of sperm sorting research is the feasibility of using smartphones in combination with OTC for home-based point-of-care devices for continuous monitoring of sperm samples. Recent work in this area has paved the way for simple automation of multi-step procedures. This includes robust sperm sorting on a single chip, integrating on-chip imaging with microchips for real-time process monitoring, advanced culture conditions, and eliminating processes which decrease sperm quality. The field of microfluidics has evolved to a point where a simplified multistage multi-compartment automated system could be designed to handle the entire volume of single ejaculate from the point after sample collection to fusion with the oocyte. Microfluidics is a crucial step in the pathway to 'affordable science' since its earliest application in sperm research.

Microfluidic devices offer an alternative to currently available technologies and clinical procedures for sperm sorting, making the technology more accessible and affordable for the consumer with potential for over-the-counter testing. In-home testing options offer privacy, convenience, and accessibility to consumers. One product currently on the market is the SpermCheck Fertility home sperm test. This FDA-approved test, available for a suggested retail price of US $39.99, is able to distinguish a normal versus a sub-fertile sperm count, claiming 98% accuracy with results comparable to laboratory testing results. The product includes a sperm collection and transfer device and the

Table 2. Comparison of various on-chip imaging technologies for sperm studies

Acquisition method	Imaging setup order (from illumination to imaging sensor)	Frame rate- dependency factor and demonstrated fps	Field of view/mm^2	Lateral Resolution limit (μm)	Image sensor pixel size (μm)	Temporal resolution	Refs
LUCAS (lensless ultra wide-field cell monitoring array platform based on shadow imaging)	LED–sample–image sensor	Depends on the type of CCD/CMOS usually >20 fps	100	0.225	10	Moderate to excellent depending on sensor type	[52]
NSOM (near-field optical scanning-based microscope)	Tungsten light–aperture–sample–CCD	Speed of scanning	–	0.15	–	Low	[53]
OFM (optofluidic microscopy)	Epi-illumination–sample–aperture–CCD/photodiode	Speed of sample/data acquisition	50	0.5	20	Moderate	[54]
SROFM (sub-pixel resolving optofluidic microscopy)	Illumination–sample–CMOS	Image acquisition of ~1300 high-resolution images/sec with 7500 fps CMOS sensor	24	0.75	2.2	Excellent	[55]
HOM (holographic optofluidic microscopy)	LED–aperture–sample–CMOS	Determined by region of interest in the sensor, 5–50 fps	24	<1	2.2	High	[56]
HOT (holographic optofluidic tomography)	LED–aperture–sample–CMOS	~5 fps	24	Lateral <1 Axial <4	2.2	Low	[56]
SPSM (sub-pixel perspective sweeping microscopy)	LED–sample–image sensor	Speed of raster scan ~10 fps	24	0.66	2.2	Low	[57]
SPMM (sub-pixel motion microscopy)	Ambient light/green LED–sample–image sensor	20–180 fps depending on ROI	24	0.5–0.95	2.2	Low	[58]

appropriate testing solutions. The system allows sperm detection above a normal threshold of 20 million sperm/ml based on the concentration of a protein found exclusively in the head of mature sperm (SpermCheck; http://www.spermcheck.com/fertility/). The Fertell male fertility test, which is currently unavailable on the market, was promoted to measure the concentration of motile sperm which are able to swim through a warmed chemical solution representing cervical fluid. The device indicated whether or not the number of motile sperm meets a 10 million/ml threshold (Fertell, Kokepelli Technologies; http://www.fertilityformen.com/products_fertell.php). The Micra is a 200X LED-illuminated microscope device intended for home semen analysis, available on the market for approximately US $70. The product includes collection materials and microscope slides for the user to evaluate liquefaction, semen volume, and sperm count and motility (Micra, Kokepelli Technologies; http://fertilityformen.com/products_micra.php). Microfluidic devices, however, have yet to be widely commercialized for the purpose of in-home sperm sorting.

Concluding remarks and future perspectives

Microfluidic lab-on-a-chip devices have been proven to be effective in both (i) analyzing a wide range of sperm functions and (ii) selecting progressive motile sperm from a mixture of seminal plasma, non-reproductive cells, mature and immature spermatozoa, non-specific debris, and various microorganisms to improve IVF outcome. Conventional methods for sperm sorting can induce DNA damage,

Box 1. Applications: single-sperm genomics and sperm-driven robotics

Microfluidics offers the ability to analyze or process sperm in a single accurate, parallelized, high-throughput device. Microfluidic technology was recently applied to single-cell whole-genome amplification for the purpose of analyzing recombination and mutation in human sperm cells [59]. Purification and separation of sperm from environmental contaminants is crucial for such sensitive assays. These assays are also sensitive to contamination from reagents used for analysis. By performing the amplification process with microfluidic chips, the reaction volume and sample contamination were reduced by ~1000-fold, thus improving the performance and accuracy of the process. The use of microfluidic devices also allows parallelization of the amplification process: the device randomly separates a sperm sample into 48 chambers such that approximately half of the chambers contain a single cell. Each aliquot is then subjected to a parallel pipeline of cell lysis, neutralization, and whole-genome amplification, yielding large numbers of high-quality genome amplification products which can be used with confidence for subsequent genomic analysis (Figure IA).

Sperm cells were recently utilized to create micro-bio-robots by trapping them into hollow microtubes [60]. These microrobots were driven by sperm flagella and were guided in microfluidic channels. By integrating thin magnetic material into the microtube and applying an external magnetic field, paths of sperm-robots were controlled in a contactless manner. The effects of several design parameters such as temperature, microtube radius, and penetration length of sperm inside the tube were evaluated. Separation of a selected sperm-robot from a pool of sperm-robots and normal sperm cells was performed in a microfluidic platform. A micro-bio-robot is formed by coupling a single sperm to a microtube. An external magnetic field is applied to control the orientation and motion trajectory, as expressed by the red arrows (Figure IB,C) [60]. More recently, transparent microtubes of diameters 10–45 μm were fabricated by the same research group using rolled-up transparent silicon oxide/dioxide nanomembranes and were utilized to study sperm dynamics in tubular confinements [61]. The effects of tube diameter on the velocity, directionality, and linearity of sperm were investigated. In addition to clinical and basic science applications, microfluidics can also serve as a platform for bio-games utilizing such sperm-robots.

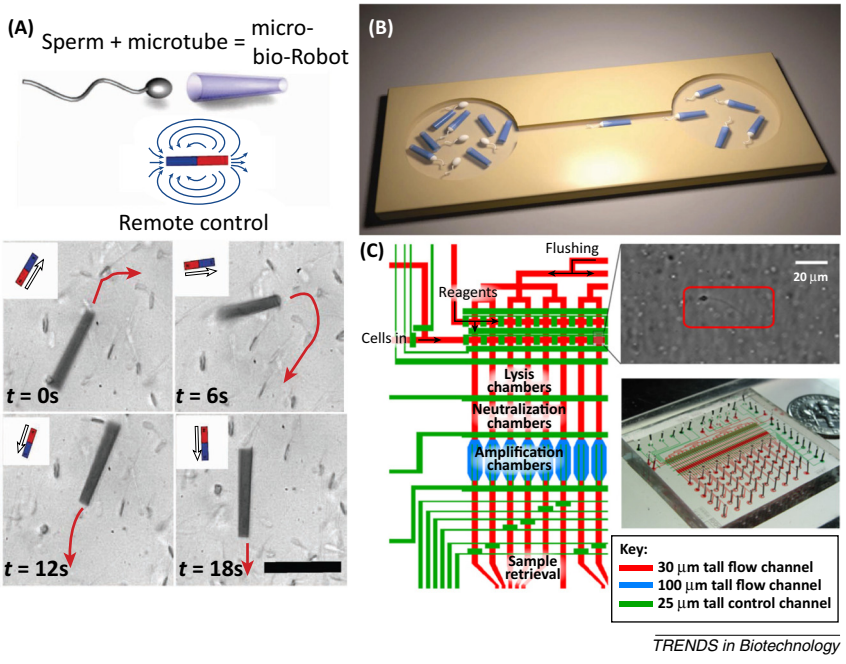

Figure I. **(A)** A schematic of the microfluidic device showing isolation of a single sperm (image) and the parallel amplification pipeline. The control channels are filled with green dye and flow channels are filled with red dye to visualize fluid flow. Reproduced, with permission, from [59]. **(B)** A micro-bio-robot formed by coupling a single sperm to a microtube. An external magnetic field is applied to control the orientation and motion trajectory, as indicated by the red arrows. **(C)** Separation of micro-bio-robots from uncoupled sperm cells and microtubules thorough a microchannel using external magnetic control. Reproduced, with permission, from [60].

Box 2. Imaging technologies integrated for microfluidic sperm research

Recent advances in image sensors, charge-coupled devices (CCD), and complementary metal oxide semiconductors (CMOS), have contributed to the development of field-portable, digital, on-chip microscopic technology. Several on-chip imaging techniques and technologies [52–58,62–64] have emerged since the first work on microfluidic shadow-imaging with CCD sensors to visualize *Caenorhabditis elegans* [63].

The CMOS sensor is preferred over CCDs for point-of-care sperm research because it is low in cost, gives a higher-resolution image, and has low heat dissipation [65]. A single white LED light source was conventionally used for on-chip imaging purposes. Image resolution was improved using multi-colored illumination and shorter wavelength (UV range) illumination obtained by tilting or shifting the source. Another novel illumination method was presented using an LED-based Google Nexus S smartphone display to illuminate a sample. The images acquired by the CMOS sensor were analyzed by a non-iterative super-resolution algorithm for automated processing [57].

An imaging platform, known as lensless ultra wide-field cell monitoring array platform based on shadow imaging (LUCAS), was developed to simultaneously image over 50 000 cells within a homogenous solution over an area of approximately 10 cm^2 [52]. The LUCAS system is shown to be scalable because the field of view depends entirely on the sensor size. The portable imaging platform has been also successfully integrated for microfluidic applications (CD4 count, AIDS.gov; https://www.aids.gov/hiv-aids-basics/just-diagnosed-with-hiv-aids/understand-your-test-results/cd4-count/[66]).

Recently, different spiral motility patterns of human and horse sperm cells were studied using a dual-view 3D tracking setup [67]. An entirely new swimming pattern of sperm having at least 3–20 rotations/s was observed [68] (Figure I). This research demonstrates the ability of the imaging system to perform microscopic imaging in 3D and to acquire video at a high frame rate of 90–140 frames/s.

The future direction of imaging technologies for sperm research will be in improving not only the lateral aspect of the spatial resolution but also the axial and temporal resolutions. Velocity analysis of sperm is crucial in identifying the healthy sperm which have the greatest potential of fusing with the oocyte for *in vitro* fertilization. Healthy and progressive motile human sperm have an inherent average path velocity of ~74 μm/s. SPMM and dual-view lens-free platform emerge as clear preferences for motile sperm cell tracking because these platforms can achieve the necessary frame rate (see Table 2 in main text).

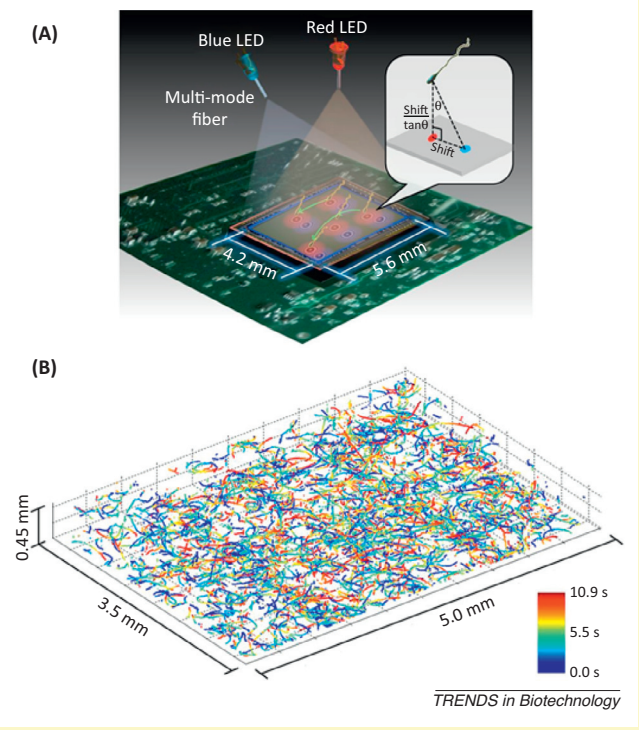

Figure I. (A) Dual-view 3D tracking of human sperm cells with two partially-coherent blue and red LEDs simultaneously illuminating the sample of interest. **(B)** A sample solution of 7.9 μl containing 1575 sperm cells was tracked with the CMOS sensor at 92 fps. Reproduced, with permission, from [68].

require labor-intensive procedures, and often yield low purity. There has been an increasing effort to develop easy-to-use, disposable, inexpensive, and high-throughput microfluidic platforms, 'labs-on-a-chip', which require a relatively small sperm sample for progressive motile sperm sorting, and may potentially be used in clinical settings for ART. In addition, such microfluidic platforms provide standardized sperm-sorting capabilities with minimum reliance on operator skills. These microfluidic sperm assays are mainly driven by self-actuation of sperm or by the addition of chemoattractant gradients, shear flows, thermotactic forces, or a combination of these. Among these microdevices, chemoattractant-driven and passively driven technologies often require no external power source or control. Advances in this field also enable applications in (i) wildlife conservation to maintain endangered species population, (ii) high-throughput single-sperm genomics to analyze recombination and mutation among sperm cells, and (iii) sperm-driven robotics (Box 1). In addition, imaging approaches are important for physicians and users to extract more comprehensive and quantitative data on a sample of interest (Box 2). Among present imaging technologies, SPMM and the dual-view lens-free platform have advantages over other technologies for motile sperm tracking. Devices currently on the market fail to take full advantage of the recent developments in microfluidic technology. OTC and smartphone imaging show promise for translating microfluidic technologies to point-of-care applications. These advances open the way for compact, simple, disposable, and inexpensive platforms that require minimum user input to analyze sperm quality at home. Improvements in microfluidic technology will greatly improve upon current point-of-care ART, ultimately making ART more affordable and accessible worldwide for couples affected by male-factor infertility.

References

1 WHO Programme of Maternal and Child Health and Family Planning Unit (1991) *Infertility: A Tabulation of Available Data on Prevalence of Primary and Secondary Infertility*, World Health Organization
2 Raymond, J.G. (1993) *Women as Wombs: Reproductive Technologies and the Battle over Women's Freedom*, Harper Collins
3 Frey, K. (2010) Male reproductive health and infertility. *Primary Care* 37, 643–652
4 Steptoe, P.C. and Edwards, R.G. (1978) Birth after the reimplantation of a human embryo. *Lancet* 2, 366
5 Palermo, G. *et al.* (1992) Pregnancies after intracytoplasmic injection of single spermatozoon into an oocyte. *Lancet* 340, 17–18
6 Rajfer, J. (2006) Freeze that sperm. *Rev Urol* 8, 43–44
7 Rajfer, J. (2006) Sperm health in the aging male. *Rev Urol* 8, 87
8 Rajfer, J. (2006) Fertility. *Rev Urol* 8, 235–236
9 O'Brien, J.K. *et al.* (2009) Application of sperm sorting and associated reproductive technology for wildlife management and conservation. *Theriogenology* 71, 98–107

10 Hansen, P. (2014) Current and future assisted reproductive technologies for mammalian farm animals. In *Current and Future Reproductive Technologies and World Food Production* (Lamb, G.C. and DiLorenzo, N., eds), pp. 1–22, Springer
11 Lemma, A. (2011) Effect of cryopreservation on sperm quality and fertility. In *Artificial Insemination in Farm Animals* (Manafi, M., ed.), pp. 191–216, InTech
12 Whitesides, G.M. (2006) The origins and the future of microfluidics. *Nature* 442, 368–373
13 Sackmann, E.K. *et al.* (2014) The present and future role of microfluidics in biomedical research. *Nature* 507, 181–189
14 Psaltis, D. *et al.* (2006) Developing optofluidic technology through the fusion of microfluidics and optics. *Nature* 442, 381–386
15 Boomsma, C.M. *et al.* (2007) Semen preparation techniques for intrauterine insemination. *Cochrane Database Syst. Rev.* 2007, CD004507
16 Henkel, R.R. and Schill, W.B. (2003) Sperm preparation for ART. *Reprod. Biol. Endocrinol.* 1, 108
17 Zini, A. *et al.* (2000) Influence of semen processing technique on human sperm DNA integrity. *Urology* 56, 1081–1084
18 Cooper, T.G. *et al.* (2010) World Health Organization reference values for human semen characteristics. *Hum. Reprod. Update* 16, 231–245
19 O'Connell, M. *et al.* (2002) The effects of cryopreservation on sperm morphology, motility and mitochondrial function. *Hum. Reprod.* 17, 704–709
20 Lopez-Garcia, M.D. *et al.* (2008) Sperm motion in a microfluidic fertilization device. *Biomed. Microdevices* 10, 709–718
21 Gurkan, U.A. *et al.* (2012) Smart interface materials integrated with microfluidics for on-demand local capture and release of cells. *Adv. Healthc. Mater.* 1, 661–668
22 Gurkan, U.A. *et al.* (2012) Emerging technologies for assembly of microscale hydrogels. *Adv. Healthc. Mater.* 1, 149–158
23 Gervais, L. *et al.* (2011) Microfluidic chips for point-of-care immunodiagnostics. *Advanced Materials* 23, H151–H176
24 Yager, P. *et al.* (2008) Point-of-care diagnostics for global health. *Annu. Rev. Biomed. Eng.* 10, 107–144
25 Tasoglu, S. *et al.* (2012) Transient spreading and swelling behavior of a gel deploying an anti-HIV topical microbicide. *J. Nonnewton. Fluid Mech.* 187/188, 36–42
26 Tasoglu, S. *et al.* (2011) The consequences of yield stress on deployment of a non-Newtonian anti-HIV microbicide gel. *J. Nonnewtonian Fluid Mech.* 166, 1116–1122
27 Tasoglu, S. *et al.* (1994) The effects of inhomogeneous boundary dilution on the coating flow of an anti-HIV microbicide vehicle. *Phys. Fluids* 23, 093101
28 Tasoglu, S. *et al.* (1994) Transient swelling, spreading, and drug delivery by a dissolved anti-HIV microbicide-bearing film. *Phys. Fluids* 25, 031901
29 Verpoorte, E. (2002) Microfluidic chips for clinical and forensic analysis. *Electrophoresis* 23, 677–712
30 Chovan, T. and Guttman, A. (2002) Microfabricated devices in biotechnology and biochemical processing. *Trends Biotechnol.* 20, 116–122
31 Beebe, D.J. *et al.* (2002) Physics and applications of microfluidics in biology. *Annu. Rev. Biomed. Eng.* 4, 261–286
32 Zare, R.N. and Kim, S. (2010) Microfluidic platforms for single-cell analysis. *Annu. Rev. Biomed. Eng.* 12, 187–201
33 Rizvi, I. *et al.* (2013) Flow induces epithelial-mesenchymal transition, cellular heterogeneity and biomarker modulation in 3D ovarian cancer nodules. *Proc. Natl. Acad. Sci. U.S.A.* 110, E1974–E1983
34 Tasoglu, S. *et al.* (2013) Manipulating biological agents and cells in micro-scale volumes for applications in medicine. *Chem. Soc. Rev.* 42, 5788–5808
35 Wang, S. *et al.* (2014) Micro-a-fluidics ELISA for rapid CD4 cell count at the point-of-care. *Sci. Rep.* 4, 3796
36 Zhang, X. *et al.* (2011) Lensless imaging for simultaneous microfluidic sperm monitoring and sorting. *Lab Chip* 11, 2535–2540
37 Tasoglu, S. *et al.* (2013) Exhaustion of racing sperm in nature-mimicking microfluidic channels during sorting. *Small* 9, 3374–3384
38 Asghar, W. *et al.* (2014) Selection of functional human sperm with higher DNA integrity and fewer reactive oxygen species. *Adv. Healthc. Mater.* 3, 1671–1679
39 Nosrati, R. *et al.* (2014) Rapid selection of sperm with high DNA integrity. *Lab Chip* 14, 1142–1150
40 Kricka, L.J. *et al.* (1993) Applications of a microfabricated device for evaluating sperm function. *Clin. Chem.* 39, 1944–1947
41 Xie, L. *et al.* (2010) Integration of sperm motility and chemotaxis screening with a microchannel-based device. *Clin. Chem.* 56, 1270–1278
42 Ma, R. *et al.* (2011) In vitro fertilization on a single-oocyte positioning system integrated with motile sperm selection and early embryo development. *Anal. Chem.* 83, 2964–2970
43 Ko, Y-J. *et al.* (2012) Separation of progressive motile sperm from mouse semen using on-chip chemotaxis. *Anal. Sci.* 28, 27–32
44 Cho, B.S. *et al.* (2003) Passively driven integrated microfluidic system for separation of motile sperm. *Anal. Chem.* 75, 1671–1675
45 Seo, D-B. *et al.* (2007) Development of sorting, aligning, and orienting motile sperm using microfluidic device operated by hydrostatic pressure. *Microfluid. Nanofluid.* 3, 561–570
46 Chen, Y-A. *et al.* (2010) Analysis of sperm concentration and motility in a microfluidic device. *Microfluid. Nanofluid.* 10, 59–67
47 Chen, C-Y. *et al.* (2013) Sperm quality assessment via separation and sedimentation in a microfluidic device. *Analyst* 2013, 4967
48 Li, Z. *et al.* (2014) The construction of an interfacial valve-based microfluidic chip for thermotaxis evaluation of human sperm. *Biomicrofluidics* 8, 024102
49 Koyama, S. *et al.* (2006) Chemotaxis assays of mouse sperm on microfluidic devices. *Anal. Chem.* 78, 3354–3359
50 Horning, M.P. *et al.* (2014) A paper microfluidic cartridge for automated staining of malaria parasites with an optically transparent microscopy window. *Lab Chip* 14, 2040–2046
51 Chung, Y. *et al.* (2006) Microscale integrated sperm sorter. *Methods Mol Biol* 321, 227–244
52 Ozcan, A. and Demirci, U. (2008) Ultra wide-field lens-free monitoring of cells on-chip. *Lab Chip* 8, 98–106
53 Betzig, E. *et al.* (1986) Near field scanning optical microscopy (NSOM): development and biophysical applications. *Biophys. J.* 49, 269–279
54 Heng, X.H.X. *et al.* (2005) Optofluidic microscopy. In *Lasers and Electro-Optics, 2005* (Vol. 3), pp. 2154–2156, IEEE
55 Zheng, G. *et al.* (2010) Sub-pixel resolving optofluidic microscope for on-chip cell imaging. *Lab Chip* 10, 3125–3129
56 Bishara, W. *et al.* (2012) Lensfree optofluidic microscopy and tomography. *Ann. Biomed. Eng.* 40, 251–262
57 Zheng, G. *et al.* (2011) The ePetri dish, an on-chip cell imaging platform based on subpixel perspective sweeping microscopy (SPSM). *Proc. Natl. Acad. Sci. U.S.A.* 108, 16889–16894
58 Lee, S.A. *et al.* (2012) On-chip continuous monitoring of motile microorganisms on an ePetri platform. *Lab Chip* 12, 2385–2390
59 Wang, J. *et al.* (2012) Genome-wide single-cell analysis of recombination activity and de novo mutation rates in human sperm. *Cell* 150, 402–412
60 Magdanz, V. *et al.* (2013) Development of a sperm-flagella driven micro-bio-robot. *Adv. Mater.* 25, 6581–6588
61 Magdanz, V. *et al.* (2014) Sperm dynamics in tubular confinement. *Small* Published online October 30, 2014. http://dx.doi.org/10.1002/smll.201401881
62 Pang, S. *et al.* (2011) Fluorescence microscopy imaging with a Fresnel zone plate array based optofluidic microscope. *Lab Chip* 11, 3698–3702
63 Lange, D. *et al.* (2005) A microfluidic shadow imaging system for the study of the nematode *Caenorhabditis elegans* in space. *Sens. Actuators B* 107, 904–914
64 Heng, X. *et al.* (2006) Optofluidic microscopy – a method for implementing a high resolution optical microscope on a chip. *Lab Chip* 6, 1274–1276
65 Seo, S. *et al.* (2008) Multi-color LUCAS: lensfree on-chip cytometry using tunable monochromatic illumination and digital noise reduction. *Cell. Mol. Bioeng.* 1, 146–156
66 Moon, S. *et al.* (2009) Integrating microfluidics and lensless imaging for point-of-care testing. *Biosens. Bioelectron.* 24, 3208–3214
67 Su, T.W. *et al.* (2013) Sperm trajectories form chiral ribbons. *Sci. Rep.* 3, 1664
68 Su, T-W. *et al.* (2012) High-throughput lensfree 3D tracking of human sperms reveals rare statistics of helical trajectories. *Proc. Natl. Acad. Sci. U.S.A.* 109, 16018–16022